

THD Minimization under Low Switching Frequency for Superior Two Level Three Phase Inverter Performance

M. Chaitanya Krishna Prasad^{1*}, Dr. Vinesh Agarwal² and Dr. Ashish Maheshwari³

¹Research scholar, Electrical Engineering, Sangam University, Bhilwara; chaitanyaprasad92@gmail.com

²Professor, Electrical Engineering, Sangam University, Bhilwara, vinesh.agarwal@sangamuniversity.ac.in

³Lecturer, Electrical Engineering, Government Polytechnic, Daman, ashish_maheshwari1987@yahoo.co.in

*Correspondence: M. Chaitanya Krishna Prasad; chaitanyaprasad92@gmail.com; +91-9160417708

ABSTRACT- The total number of switching pulses permitted in one-quarter of the fundamental-cycle of an inverter is restricted due to the restrictions of switching losses in high-power inverter devices. The elimination of major low-order dominating harmonics using SHEPWM (Selective Harmonic Elimination) is suggested in this research paper. The positive or negative voltage transition at the instant where fundamental voltage has the greatest positive slope distinguishes the various types of waveforms. Due to the switching loss limitations, two forms of the pole voltage PWM waveforms i.e., type A, type B, were studied in this research at lower pulse number ($P = 5$). For a two-level three-phase inverter, an ideal Pulse Width Modulated (PWM) waveform is developed for whole modulation index range in terms of least total harmonic distortion (THD). MATLAB simulation and practical experiments are performed for a two-level inverter to support the theoretical analysis and results.

Keywords: Two level Inverter, Selective Harmonic Elimination, Optimization Algorithms, PWM formulations, Iterative techniques.

ARTICLE INFORMATION

Author(s): M. Chaitanya Krishna Prasad, Dr. Vinesh Agarwal and Dr. Ashish Maheshwari;

Received: 22/10/2022; **Accepted:** 13/12/2022; **Published:** 25/12/2022;

e-ISSN: 2347-470X;

Paper Id: IJEER2210-11;

Citation: 10.37391/IJEER.100476

Webpage-link:

www.ijeer.forexjournal.co.in/archive/volume-10/ijeer-100476.html



Publisher's Note: FOREX Publication stays neutral with regard to Jurisdictional claims in Published maps and institutional affiliations.

1. INTRODUCTION

Voltage Source Inverters (VSIs) are typically used to generate sinusoidal three phase wave form from fixed DC source for the use in the motor drives [1]. Voltage Source Inverters (VSIs) with high power PWM are extensively used in residential and industrial applications such as the motor drives, STATCOM, FACTS devices, APFs (Active power filters) [2],[3]. In low power applications, a greater pulse number ($P=2N+1$) is used to improve the quality of an inverter output line voltage (Here, 'N' specifies total count of the switching instants present in each quarter cycle of the fundamental waveform) [4], [5]. Because of lower device switching loss, low switching frequency operation improves inverter efficiency [6]. However, due to increased switching losses of power semiconductor devices, low frequency device switching is preferable at higher power levels [7]. Lower order voltage harmonics cause pulsing torque, which can cause severe damage to motor drive control system[8],[9]. At low switching frequency, Pole voltage waveform of a voltage source inverter (VSI) has odd harmonics around the fundamental waveform. Various PWM techniques, such as the traditional SPWM, SVPWM, and SHEPWM, have been proposed to improve inverter performance [10], [11]. The

PWM modulation approach determines the inverter's performance. In the last three decades, several modulation approaches have been documented in [12-16]. The primary modulation strategies are STPWM (sine triangular pulse width modulation) [17], SVPWM (Space Vector pulse width modulation) [18], SHEPWM (Selective Harmonic Elimination Pulse Width Modulation) [19].

The primary purpose of SHEPWM approach is to solve nonlinear transcendental equations, that might result in no solution, a single solution, or several solutions for a given modulation index value. [20-21]. Several strategies for solving nonlinear equations with trigonometric components in order to determine the best switching angles have been developed using PSO (particle swarm optimization) [22] and GA (Genetic algorithm) [23] have been proposed for calculating the switching angles required to operate the multilevel inverters. However, there are no simple ways for determining the parameters needed for the aforementioned optimization strategies. To solve the equations, numerical iterative techniques for example the Newton Raphson method [24], [25], resultant theory [26], [27] are applied.

The difficulty with resultant theory is the complexity of resulting polynomial solution develops as the ordering of the transcendental equations rises. In actuality, the resulting theory is limited to six switching angles for equal and unequal DC sources, respectively. However, in the case of the NR approach, the convergence of the solution to the global minimum is dependent on the selection of appropriate starting switching angle values. Other options offered include bee algorithm [28], Groebner bases algorithm [29], neural networks [30] and harmony search [31] to obtain the optimum switching angles. In the reference [32] offered solutions for multilevel converters with equal DC sources using a genetic algorithm. However, the

solution for switching angles for particular modulation index was not explored. Another method based on PSO (Particle Swarm Optimization) employing equal DC sources is used to seven and eleven level inverters to remove only non-triple harmonics [33]. Despite the fact that all potential sets of solutions are identified, the solution space cannot be enlarged for all modulation index ranges. To widen the modulation range, the same problem is overcome by incorporating dissimilar DC sources [34], Non symmetrical modulation [35] and combination of dissimilar DC voltage and non-symmetrical modulation concurrently [36]. The pole voltages are classified according to their kind (*type A* or *type B*) as well as pulse number (P) that is dependent on number of the switching intervals (N) in the quarter of a fundamental cycle. Positive and negative voltages transition at the position of zero crossing, as well as a positive slope of a fundamental voltage, distinguishes *type A* and *type B* pole voltage waveforms. The accuracy of the *type A* and *type B* PWM waveforms for minimizing line current total harmonic distortion at $P=5$ and $P=7$ of two level [37] and three level [38] inverters has been tested. However, the inquiry produced an ideal solution for the whole modulation index range when just solution set A both for *type A* as well as *type B* PWM waveforms were considered.

The study calculates optimum switching angles of *type A* as well as *type B* pole voltages based on the least voltage waveform distortion (V_{WTHD}) for $P=5$, i.e. $N=2$. Out of four solution sets only one set outperforms the others at each modulation index. As a result, a Combined Optimum PWM (CO-PWM) is presented, which takes a best of the various options available with reference to lowest harmonic distortion for line current (I_{THD}) and line voltage (V_{WTHD}). The rest of this paper is arranged as follows. *Section 2* will discuss the *type A* and *type B* waveform formulations, as well as the specifics of four solution set outcomes computed using the Genetic Algorithm for a two-level inverter. *Section 3* will explore a comparative evaluation based on analytical and simulation findings between suggested optimum PWM (CO-PWM) and SHE-PWM for the identical number of the switching angles each quarter cycle ($N=2$). *Section 4* analyze the results of experiments and compares three PWM approaches, CO-PWM, SHE-PWM, and ST-PWM, with considerations of (V_{WTHD})

weighted overall harmonic distortion of the inverter line voltage. Finally, *Section 5* presents a conclusion.

2. Type-A & Type-B Pulse Width Modulation Waveforms

Figures 1(a) and *(b)* show R Phase voltage *type-A* as well as *type-B* waveforms with reference to a DC bus voltage midpoint for two levels of V_{SI} at $P=5$. Both waveforms in *figure 1* have two switching angles α_1 and α_2 each quarter wave, the values of which may be chosen to reduce V_{WTHD} while maintaining the required peak fundamental voltage. The switching transition of $-V_{dc}/2$ to $+V_{dc}/2$ at positive zero crossing, i.e. $\theta = 0^\circ$, identifies *type A* waveform, whereas *type B* waveform includes switching from $+V_{dc}/2$ to $-V_{dc}/2$ at $\theta = 0^\circ$ [31]. Furthermore, each of the aforementioned waveforms preserve HWS (Half Wave Symmetry) as well as QWS (Quarter Wave Symmetry) for every fundamental cycle if the requirements indicated in *eq. (1)* and *(2)* are satisfied. As the result, there is no even number harmonics present in the line voltage output of an inverter [39].

$$V_{RO}(\theta) = V_{RO}(\theta + 180) \quad (1)$$

$$V_{RO}(\theta_m - \theta) = V_{RO}(\theta_m + \theta) \quad (2)$$

Where, θ_m is the instant, when the R-phase voltage reaches its maximum positive or negative value. The three phase pole voltages has to be symmetric in accordance with the *equation (3)* in order to achieve balanced output for tripled harmonic cancellation

$$V_{RO}(\theta) = V_{YO}(\theta + 120) = V_{BO}(240 + \theta) \quad (3)$$

The maximum amplitudes of a fundamental as well as odd number harmonic components (F_{na} and F_{nb}) with $P=5$ of *type A*, *type B* waveforms are provided by *eq. (4)* and *(5)*, respectively, based on Fourier analysis

$$F_{na} = \frac{2V_{dc}}{n\pi} [1 - 2 \cos(n\alpha_1) + 2 \cos(n\alpha_2)] \quad (4)$$

$$F_{nb} = \frac{2V_{dc}}{n\pi} [-1 + 2 \cos(n\alpha_1) - 2 \cos(n\alpha_2)] \quad (5)$$

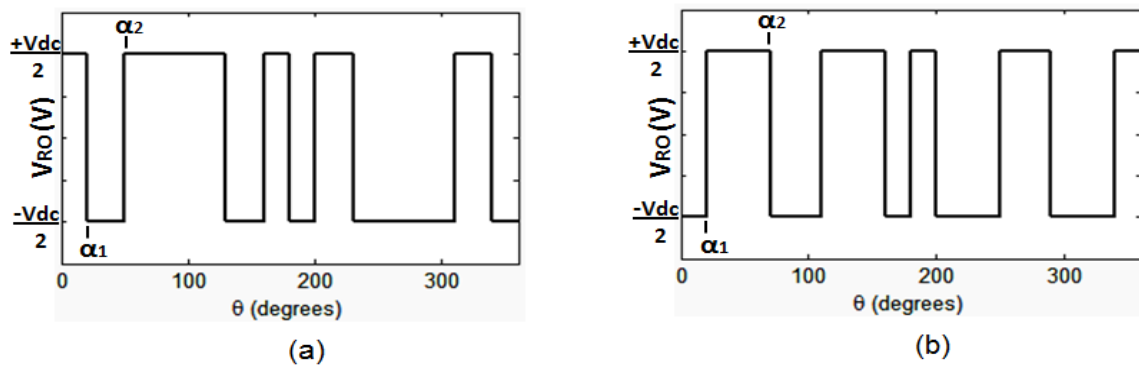


Figure 1: Two-level voltage source inverter (VSI) pole voltage waveform VRO pertaining to (a) *type-A* PWM and (b) *type-B* PWM with $N=2$.

Where, V_{dc} denotes the DC bus voltage, α_1 and α_2 denotes the independent switching angles, and n denote the harmonic order.

Off-line PWM approaches, such as the SHEPWM method with N switching angles each quarter cycle, may reduce $(N-1)$ voltage harmonics of the inverter output, while maintaining the required fundamental voltage [40]. However, eliminating some low order harmonics does not guarantee low line voltage THD [41]. Furthermore, for larger modulation indices, methods for full removal of lower harmonics may be unavailable, resulting in a higher line voltage THD value. In the case of optimum PWM, the aim is to reduce harmonic distortion of line current in inverter (I_{THD}) at low pulse number, as shown by equation (6) I_{THD} is often accepted as the overall distortion factor of motor driving loads [42-45].

$$I_{THD} = \sqrt{\frac{\sum_{n=6K+1} I_n^2}{I_1^2}} \quad K = 1, 2, 3 \dots \quad (6)$$

Fundamental RMS current is I_1 , while the n th order harmonic current is I_n . However, because line current distortion (I_{THD}) is affected by load characteristics, line-line voltage harmonic distortion (V_{WTHD}) is taken into account for reduction as specified in equation (7)

$$V_{WTHD} = \sqrt{\frac{\sum_{n=6K+1} F_n^2 / n^2}{F_1^2}} \quad K = 1, 2, 3 \dots \quad (7)$$

The RMS fundamental voltage is F_1 , while the n th order harmonic voltage is F_n . As seen in eq. (7), V_{WTHD} depends on the harmonic and fundamental voltages of the inverter output line voltage. The peak values for harmonic and fundamental voltages can be determined using the equations (4) and (5) for type A and type B respectively. To demonstrate the feasibility

of the proposed combined PWM strategy for wide operational modulation range, two different two level PWM waveforms namely *type A* & *type B* are considered in this paper. For each type of PWM waveform, optimal switching angles are achieved by solving two different sets of equations. As the equations in (4) and (5) are non-linear equations, intelligent optimization techniques [46] like genetic algorithm (GA) is used to determine the initial values of switching angles [39]. A user-friendly function in MATLAB called 'ga' is used to compute initial set of values (α_1 and α_2) to obtain multiple solutions using Newton-Raphson (NR) iterative method [40]. The syntax for 'ga' function to find minimum for function 'fun', subject to non-linear equalities and inequalities is as follows:

$$X = ga(fun, nvars, A, b, A_{eq}, B_{eq}, lb, ub, nonlcon, options)$$

A sufficient fitness function must be developed before the genetic algorithm may begin. A decent fitness function incorporates several control variables towards a single function. The goal is to reduce line voltage THD while still achieving the appropriate fundamental component at all modulation index values. As a result, the goal fitness function must be built with all these harmonics as well as fundamental Components in mind as demonstrated in eq. (8).

$$f(\alpha_1, \alpha_2) = \min \left[\left(100 \frac{F_1^* - F_1}{F_1} \right)^4 + \sum_{n=5,7 \dots}^{3N-1} \frac{1}{n} \left(\frac{F_n}{F_1} \right) \right] \quad (8)$$

$$restricted \text{ to } : 0 \leq \alpha_1 \leq \alpha_2 \leq \frac{\pi}{2} \quad (9)$$

Here, F_1^* denotes the required fundamental component and 'n' denotes harmonic order. A power of 4 and a constraint component of 100 were integrated into the fitness function to identify the primary term, which comprises the basic component from other secondary terms.

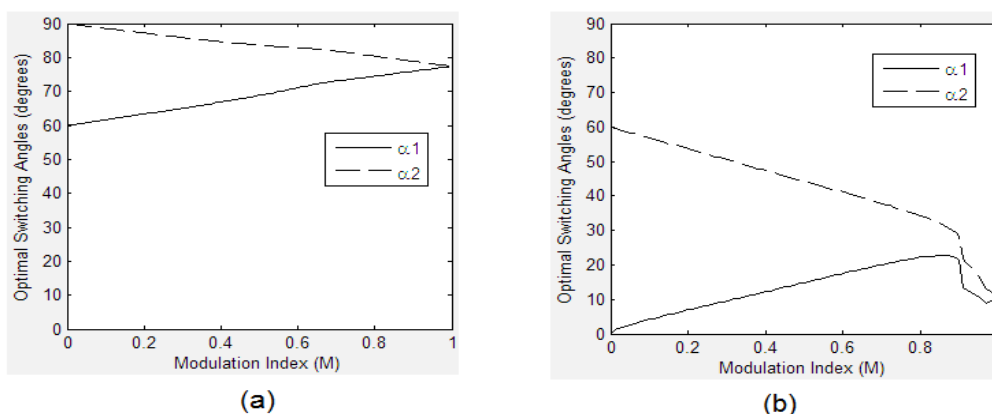


Figure 2: Optimum switching angles of type A PWM (a) solution set A and (b) solution set B

Each harmonic phrase incorporates appropriate weighting factors supplied by reciprocal of specific harmonic orders to boost the chance of low-level harmonic removal compared to higher orders [47]. While the following conditions are met, then objective function must be zero for every initial modulation index value:

- The fundamental component (F_1) equals the intended value F_1^*
- The value of total harmonic distortion obtained is minimum (or less than a threshold value).
- Switching angles adhere to the inequality restriction as specified in eq. (9).

The optimal switching angles determined using the evolutionary algorithm are then utilized as beginning Values in the Newton-Raphson iterative approach to produce numerous set of solutions of *type A* as well as *type B* PWM waveforms. The following Optimization approach is used to determine the ideal switching angles with this case study:

- (i) With the aforementioned requirements met, obtain an initial prediction about switching angles using a genetic algorithm. (Assume variable starting values are found for modulation index 'M').
- (ii) Generate an objective function 'f' and its Jacobean (J) with six switching angles of variables.

- (iii) Determine the values of 'f new' and 'Jnew' for the original switching angle values (α_{old}).
- (iv) Solve for the updated values of switching angles:
- (v) $\alpha_{new} = \alpha_{old} + J_{new} / f_{new}$
- (vi) Repeat the steps (iii) (iv) by increasing the modulation index 'M' by 0.01
- (vii) A similar technique is used to generate a full solution set by lowering the value of 'M'
- (viii) Obtain additional solution sets for varying starting switching angle values, resulting in numerous solution sets.

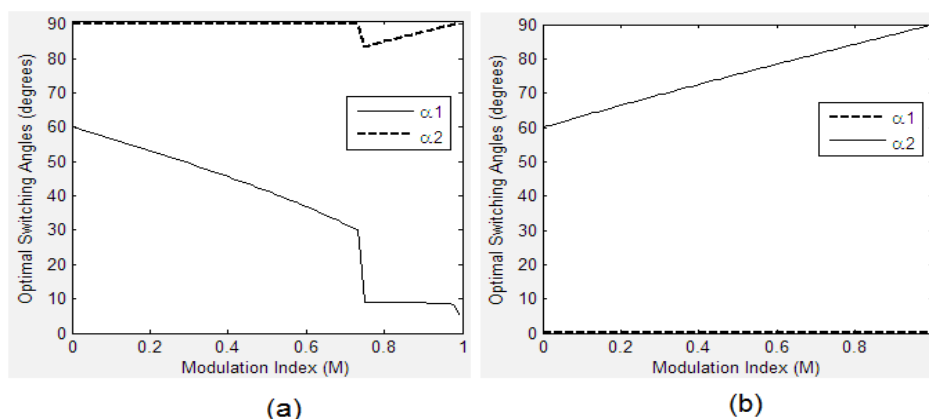


Figure 3: Optimum switching angles of type B PWM (a) solution set A and (b) solution set B

The aforementioned technique was developed for *type A* & *type B* PWM waveforms, and several solutions were discovered and reported, confirming the original hypothesis. The N-R technique is configured to run for a specific number of the iterations (In this example 100 times) in order to get Optimum solution sets. Figures 2(a) and (b) show the best switching angles of solution sets A and B for the type A PWM waveform. Figures 3(a) and (b) show two distinct solution sets for the type B PWM waveform to obtain minimal V_{WTHD} .

3. COMBINED OPTIMUM PWM (CO-PWM) WITH MINIMIZATION OF THD

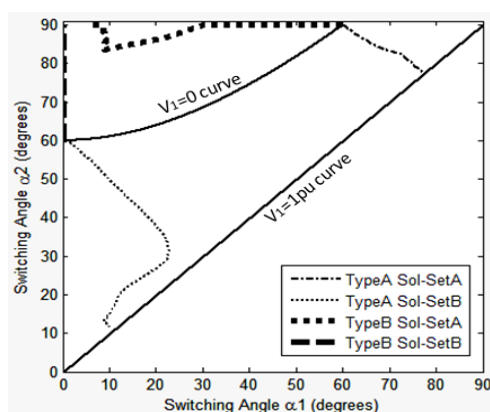


Figure 4: Four optimal switching angle set on α_2 versus α_1 plane

In Figure 4, the four possible sets of solutions for type A as well as type B waveforms were illustrated on a α_1 against α_2 plane, with the inequality restriction upon these switching angles being $0 \leq \alpha_1 \leq \alpha_2 \leq \pi/2$.

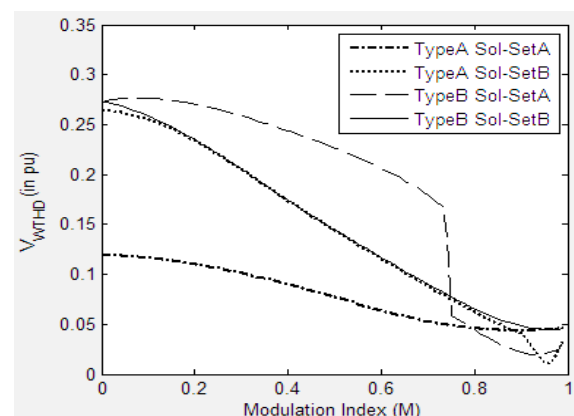


Figure 5: Analytical comparison of the V_{WTHD} corresponding to optimal type A and type B solution sets

Figure 5 depicts that simulated values for V_{WTHD} according to two separate solution sets of *type A* as well as *type B* PWM. The V_{WTHD} value for solution set A of the *type A* waveform given in figure 5 demonstrates increased performance for the range $0 \leq M \leq 0.79$. Solution set-A with *type B* waveform beats other solution sets. Finally, for any M value more than 0.935, solution set-B with *type A* waveform has the lowest V_{WTHD} value when

compared to many other solutions. As seen in *figure 5*, neither *type A* nor *type B* waveforms are better over the whole modulation index range. As a result, a Combined Optimum PWM (CO-PWM) is proposed, which adopts the best solution from the four separate solution sets previously evaluated at different modulation index values.

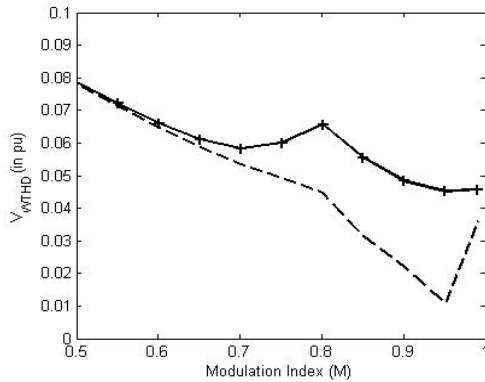


Figure 6: Optimum switching angles of proposed combined optimum PWM

Figure 6 depicts the whole set of the switching angles for the CO-PWM waveforms within a modulation range $0 \leq M \leq 1$ in 0.01 increments. Because of the extended search procedure throughout the whole solution space, the V_{WTHD} values corresponding to the CO-PWM waveform outperform the PWM presented in the literature [37]. As previously explained, it is possible to remove non triplen 5th harmonic voltages by using two switching angles for a quarter cycle, while keeping the fundamental voltage constant. The fundamental and fifth harmonic voltage peak values of SHEPWM for $N=2$ are presented in *eq. (10) and (11)* correspondingly. To calculate the switching angles α_1 and α_2 for the SHE-PWM technique, both formulas (10) as well as (11) are solved concurrently.

$$V_1 = \frac{2V_{dc}}{\pi} [1 - 2 \cos(\alpha_1) + 2 \cos(\alpha_2)] \quad (10)$$

$$V_5 = \frac{2V_{dc}}{5\pi} [1 - 2 \cos(5\alpha_1) + 2 \cos(5\alpha_2)] = 0 \quad (11)$$

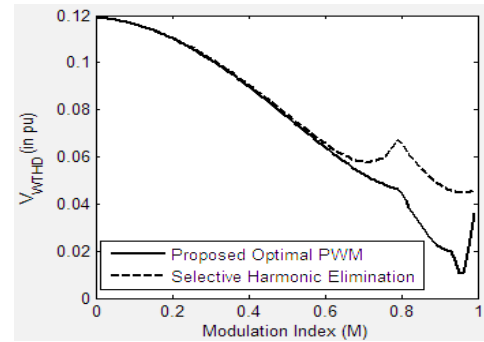


Figure 7: Comparison of the proposed combined optimum (CO-PWM) and SHEPWM in terms to theoretical values of V_{WTHD} , $P=5$

Figure 7 depicts a relative effectiveness between CO-PWM versus SHE-PWM in regards of the minimal V_{WTHD} value. As it can be shown, the CO-PWM waveform outperforms the SHEPWM approach for the modulation index values greater than 0.6. Because *type A*, *type B* and SHE-PWM waveforms have HWS and QWS symmetry, even harmonics are missing in output line voltage of inverter. PWM waveforms are also free of triplet odd harmonics because of three-phase symmetry as indicated in *eq. (3)*.

4. RESULTS OF EXPERIMENT

The suggested CO-PWM, SHE-PWM, and ST-PWM Techniques have been implemented in a two-level inverter with a fixed DC bus voltage of 30V shown in *figure 8*. As the switching power device, a 100V, 33A IRF540N n-channel MOSFET was used in the experimental prototype. The microcontroller based on the Atmega-328 is used to perform control algorithm for real time and create gate controlling signals of switching devices depending on the modulation index value. The gate control circuit contains an IR2104 high speed half wave bridge driver as well as an opto-coupler IC MCT2E to isolate the microcontroller from high DC voltage side. Prototype uses three half H-bridges for every phase of three-phase two level inverter, with gate voltage provided by an isolated Single-phase rectifier. Due to space constraints, the current study merely summarizes the experimental results. For reference, simulated waveforms and spectrums for the different PWM-techniques under consideration may be found in [48].

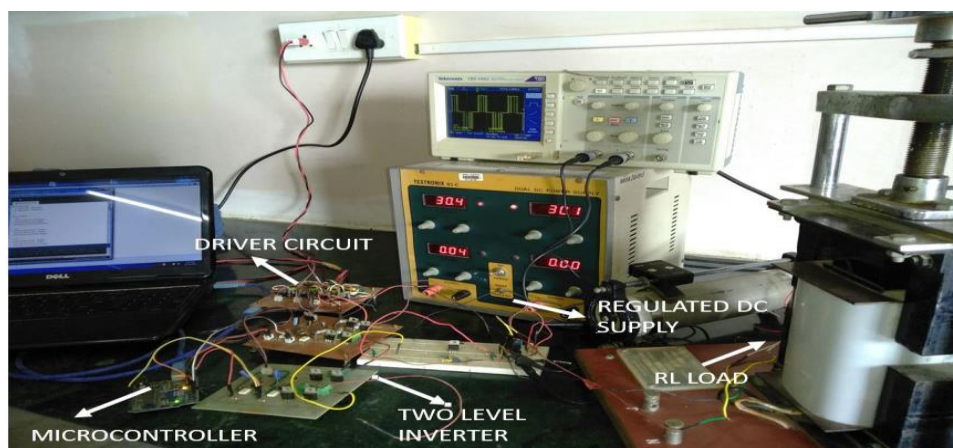


Figure 8: Experimental set up

For ease of measurement, the switching frequency was set to 250Hz, and the fundamental line-line voltage frequency was set to 50Hz. In addition, the dead-time for experimental PWM schemes was adjusted to 6 μ sec. A Tektronix TBS 1062 digital oscilloscope was used to capture the inverter output voltages and display its spectrum using the scope's FFT (Fast Fourier Transform) capability. The operational point M is set to 0.6 for the initial experimental research. *Figures 9(a), (b), (c), and (d)* show the experimental findings for the 50Hz inverter line-line voltage time function waveform for STPWM, SHEPWM, type A solution set A, and type B solution set A, respectively. *Figures 10(a), (b), (c), (d)* show the appropriate FFT spectrum

charts of an inverter line-line output voltages for the aforementioned PWM approaches. Due to the HWS as well as 3 phase symmetry, PWM waveforms omit even harmonics along with triplen odd-harmonics, as seen in *Figures 10(b), (c), and (d)* for SHE-PWM, type A solution set-A, and type B solution set-A, respectively. However, for the non-triplen odd chopping frequencies, such as P=5, phase symmetry is not preserved for the ST-PWM approach, limiting correct cancellation of triplen order amongst pole voltage harmonics [49].

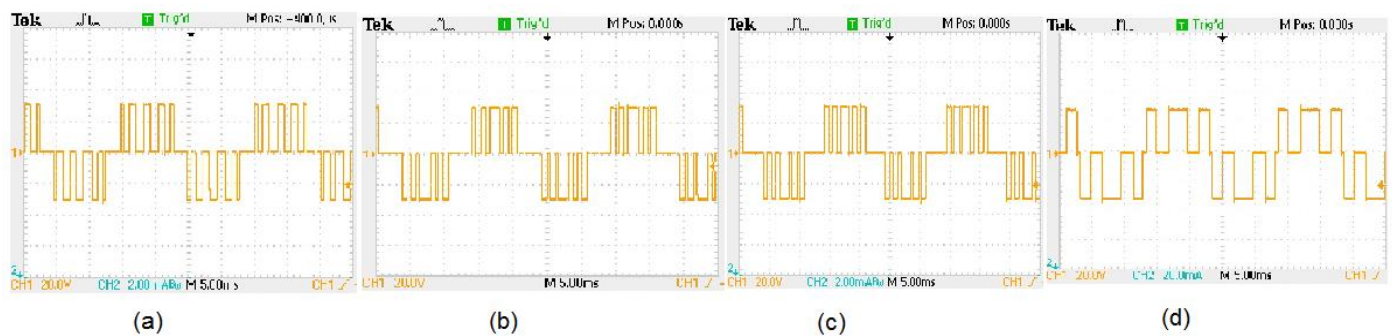


Figure 9: Measured line voltage (VRY) of (a) STPWM (b) SHEPWM (c) type A solution setA (d) type A solution setA at M=0.6, P=5. Scale:20V/div

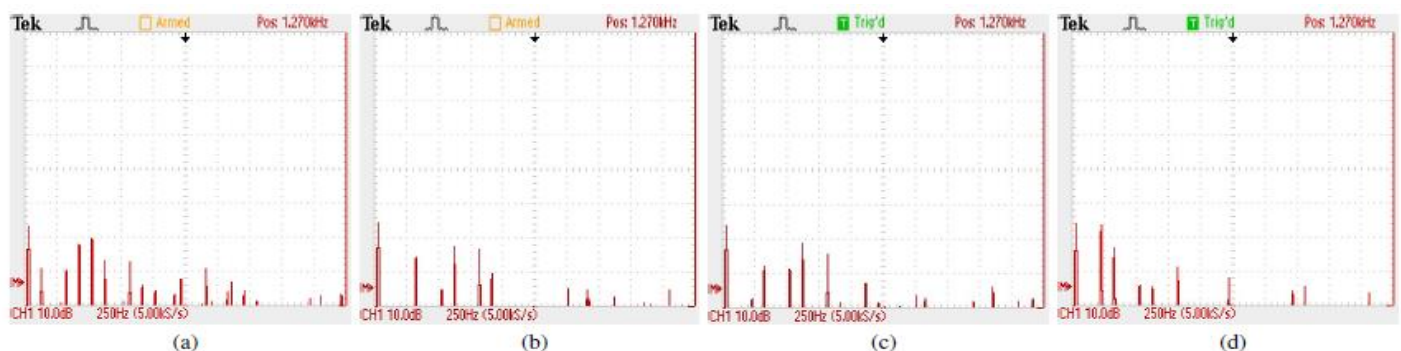


Figure 10: Measured line voltage (VRY) harmonic order of (a) STPWM (b) SHEPWM (c) type A solution setA (d) type A solution setA at M=0.6, P=5. Scale:10dB/div

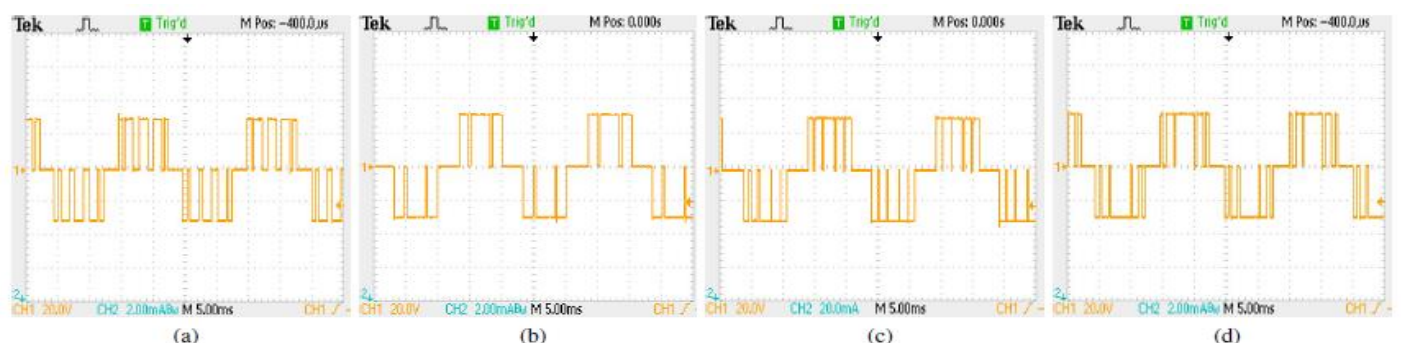


Figure 11: Measured line voltage (VRY) of (a) STPWM (b) SHEPWM (c) type A solution setA (d) type A solution setA at M=0.85, P=5. Scale:20V/div

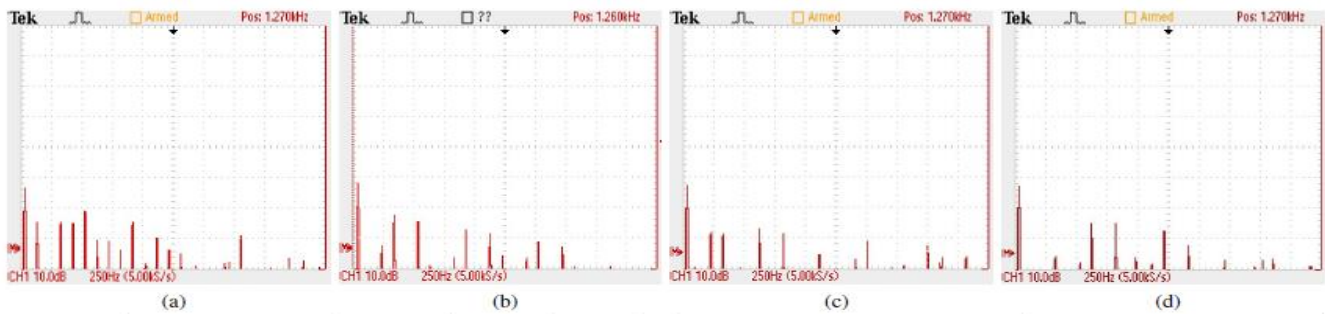


Figure 12: Measured line voltage (VRY) harmonic order of (a) STPWM (b) SHEPWM (c) type A solution set A (d) type A solution set A at $M=0.85$, $P=5$. Scale: 10dB/div

To maintain three-phase symmetry (TPS) in ST-PWM, the ratio between chopping frequency and the modulation signal frequency might be an odd-triplex multiple. Triplex-harmonic frequency components are clearly visible in the FFT spectrum shown in *figure 10(a)* for ST-PWM. The FFT analysis of SHE-PWM validates the full removal of the 5th harmonic from the inverter line voltage, as shown in *figure 10(b)*. The overall harmonic distortion for the SHE-PWM approach, on the other hand, is considerable because of high order non-zero and non-triplex harmonics.

The next experiment was performed with $M=0.85$. The findings for inverter line-line voltage waveforms related to the four distinct PWM algorithms for $P=5$ are shown in *figure 11(a)*, (b), (c), and (d). The line-line voltage harmonic spectra for SHEPWM, STPWM, type A solution set-A, and type B Solution set-A are depicted in *figures 12(a)*, (b), (c), and (d). The existence of the triplex harmonics in the ST-PWM technique is confirmed further by the experimental voltage harmonic spectrum shown in *figure 12(a)*. The harmonic spectrum of *figure 12(b)* shows that SHE-PWM fail to provide a solution to Specific 5th harmonic removal above $M=0.79$. The suggested Combined CO-PWM approach, on the other hand, finds optimal angle solutions up to six-step operation. Instead of particular removal, the CO-PWM approach assures that overall low-order harmonics are minimized at any M value. For $M=0.85$, the angles related with type B solution set-A efficiently minimize V_{WTHD} value, which is consistent with the findings given in *figure 7*.

Table 1 and *Table 2* show the optimal switching angles with line-line voltage weighted Distortion (V_{WTHD}) values with $M=0.6$ and $M=0.85$ for STPWM, SHEPWM, type A solution set-A, and type B solution set-A.

Table 1: Optimum switching angles, harmonic distortion values of $M=0.6$ for $P=5$

Modulation Techniques	Switching Angle α_1	Switching Angle α_2	Simulated V_{WTHD} Value	Measured V_{WTHD} Value
STPWM	-	-	0.1279	0.1386
SHEPWM	72.27	84.00	0.0657	0.0723
Type A PWM	71.05	82.83	0.0642	0.0693
Type B PWM	36.87	90	0.1168	0.1572

Table 2: Optimum switching angles, harmonic distortion values of $M=0.85$ for $P=5$

Modulation Techniques	Switching Angle α_1	Switching Angle α_2	Simulated V_{WTHD} Value	Measured V_{WTHD} Value
STPWM	-	-	0.1265	0.1288
SHEPWM	85.70	90.00	0.0554	0.0592
Type A PWM	75.31	79.71	0.0442	0.0468
Type B PWM	9.05	86.41	0.0312	0.0385

As previously stated, the suggested CO-PWM approach produces the lowest line-voltage distortion V_{WTHD} at $M=0.60$ and $M=0.85$, the performance for type A solutions set-A with type B solutions set-A was shown to be superior to other PWM approaches.

4.1 SHEPWM, STPWM comparison with suggested CO-PWM

Figure 13 depicts a comparison of the three PWM approaches, namely CO-PWM, SHE-PWM, and ST-PWM, based on measured V_{WTHD} values. *Tables 1* and *2*, as well as *figure 13*, clearly demonstrate that proposed CO-PWM scheme outperforms SHEPWM and STPWM for $P=5$. SHE-PWM also fails to give optimum solutions for 5th harmonic removal for said modulation index range $M \geq 0.79$. As previously stated, the suggested CO-PWM approach utilizes the optimum solution set for a particular modulation index value that seeks to minimize total harmonic distortion rather than removing specific low order harmonics. CO-PWM approach provides much lower V_{WTHD} values than SHE-PWM and ST-PWM Schemes for $M \geq 0.6$ and entire modulation index (M) ranges, respectively.

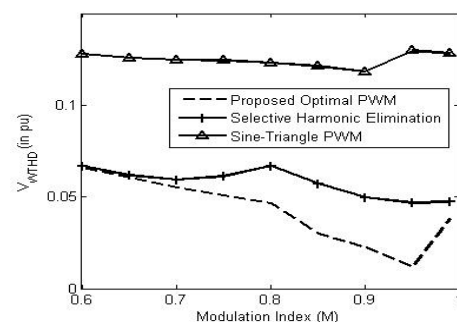


Figure 13: SHEPWM, STPWM comparison with suggested CO-PWM for simulated values of V_{WTHD} , $P=5$

However, for lower M ranges, the V_{WTHD} value for CO-PWM is somewhat lower than for SHE-PWM. As a result, as compared to ST-PWM & SHE-PWM, the combining of both *type A* as well as *type B* solution sets provides significantly higher harmonic performance.

5. CONCLUSION

This research presents a combined optimum CO-PWM strategy for enhancing the overall weighted THD of an inverter's output voltage. The GA algorithm and the NR iterative approach were used to identify four solution sets for *type A* and *type B* PWM waveform for two level inverters using two switching angles each quarter cycle. After analyzing all four alternatives, an optimal combination PWM (CO-PWM) is designed based on the preceding findings. Several simulations as well as actual experimental results are shown to validate the CO-PWM techniques improve performance when compared to the SHE-PWM and ST-PWM methods. Furthermore, at modulation index values greater than 0.6, the CO-PWM outperforms the SHE-PWM. Additionally, the CO-PWM approach produces significantly lower V_{WTHD} values than ST-PWM throughout the complete modulation index range. The research findings can be implemented in various real time applications like micro grid, electric vehicle, distributed generation, hybrid vehicle etc., to improve inverter performance.

REFERENCES

- [1] M. Hagiwara, K. Nishimura, and H. Akagi, "A medium-voltage motor drive with a modular multilevel PWM inverter," IEEE Trans. Power Electron., vol. 25, no. 7, pp. 1786-1799, Jul. 2010
- [2] F. Blaabjerg, Z. Chen, and S. B. Kjaer, "Power electronics as efficient interface in dispersed power generation systems," IEEE Trans. Power Electron., vol. 19, no. 5, pp. 1184-1194, Sept. 2004
- [3] M. Malinowski, M. P. Kazmierkowski, and A. M. Trzynadlowski, "A comparative study of control techniques for PWM rectifiers in AC adjustable speed drives," IEEE Trans. Power Electron., vol. 18, no. 6, pp. 1390-1396, Nov. 2003, pp. 2423-2430, 2011
- [4] D. Holmes and T. Lipo, Pulse width modulation for power converters: principles and practice. John Wiley and Sons, 2003
- [5] J. Holtz, "Pulsewidth modulation-a survey," IEEE Trans. Ind. Electron., vol. 39, no. 5, pp. 410-420, Oct 1992.
- [6] A. Edpuganti and A. K. Rathore, "Optimal Low Switching Frequency Pulsewidth Modulation of Nine-Level Cascade Inverter," in IEEE Transactions on Power Electronics, vol. 30, no. 1, pp. 482-495, Jan. 2015.
- [7] A. Tripathi and G. Narayanan, "Evaluation and minimization of low order harmonic torque in low-switching-frequency inverter fed induction motor drives," IEEE Trans. Ind. Appl., vol. 52, no. 2, pp. 1477-1488, March 2016
- [8] J. Song-Manguelle, J.-M. Nyobe-Yome, and G. Ekemb, "Pulsating torques in pwm multi-megawatt drives for tensional analysis of large shafts," IEEE Trans. Ind. Appl., vol. 46, no. 1, pp. 130-138, Jan 2010.
- [9] J. Song-Manguelle, S. Schroder, T. Geyer, G. Ekemb, and J.-M. Nyobe-Yome, "Prediction of mechanical shaft failures due to pulsating torques of variable-frequency drives," IEEE Trans. Ind. Appl., vol. 46, no. 5, pp. 1979-1988, Sept 2010
- [10] D. Holmes and T. Lipo, Pulse width modulation for power converters: principles and practice. John Wiley and Sons, 2003
- [11] K. A. Corzine, M. W. Wieleski, F. Peng, and J. Wang, "Control of cascaded multi-level inverters," in Electric Machines and Drives Conference, 2003. IEMDC'03. IEEE International, 2003, pp. 1549-1555
- [12] L. M. Tolbert and T. G. Habetler, "Novel multilevel inverter carrier based PWM method," in IEEE Transactions on Industry Applications, vol. 35, no. 5, pp. 1098-1107, Sept.-Oct. 1999.
- [13] H. L. Liu and G. H. Cho, "Three level space vector PWM in low index modulation region avoiding narrow pulse problem," IEEE Trans. Power Electron., vol. 8, pp. 481-486, Sept. 1994.
- [14] L. Gao and J. E. Fletcher, "A Space Vector Switching Strategy for Three-Level Five-Phase Inverter Drives," in IEEE Transactions on Industrial-Electronics, vol. 57, no. 7, pp. 2332-2343, July 2010.
- [15] M. H. Rashid, "Power Electronics Circuits, Devices and Applications", 3rd edition, Pearson Prentice Hall, 2006.
- [16] SurinKhomfoi and L. M. Tolbert, "Multilevel Power Converters", Power Electronics Handbook, Chapter 31, 2007
- [17] L. M. Tolbert and T. G. Habetler, "Novel multilevel inverter carrierbased PWM method," in IEEE Transactions on Industry Applications, vol. 35, no. 5, pp. 1098-1107, Sept.-Oct. 1999.
- [18] D. Reney, "Modeling and Simulation of Space Vector PWM Inverter," 2011 International Conference on Devices and Communications (ICDe-Com), 2011, pp. 1-4, doi: 10.1109/ICDECOM.2011.5738466.
- [19] A. Kiani Harchegani and H. Iman-Eini, "Selective harmonic elimination pulse width modulation in single-phase modular multilevel converter," The 6th Power Electronics, Drive Systems and Technologies Conference (PEDSTC2015), 2015, pp. 346-351, doi: 10.1109/PEDSTC.2015.7093299
- [20] M. Balasubramanian and V. Rajamani, "Design and Real-Time Implementation of SHEPWM in Single-Phase Inverter Using Generalized Hopfield Neural Network," in IEEE Transactions on Industrial Electronics, vol. 61, no. 11, pp. 6327-6336, Nov. 2014, doi: 10.1109/TIE.2014.2304919
- [21] G. S. Konstantinou and V. G. Agelidis, "Bipolar switching waveform: Novel solution sets to the selective harmonic elimination problem," 2010 IEEE International Conference on Industrial Technology, 2010, pp. 696-701, doi: 10.1109/ICIT.2010.5472718.
- [22] A. Kouzou et al., "Selective Harmonics Elimination for a three level diode clamped five-phase inverter based on Particle Swarm Optimization," IECON 2011 - 37th Annual Conference of the IEEE Industrial Electronics Society, 2011, pp. 3495-3500, doi: 10.1109/IECON.2011.6119874.
- [23] E. Deniz, O. Aydogmus and Z. Aydogmus, "GA-based optimization and ANN-based SHEPWM generation for two-level inverter," 2015 IEEE International Conference on Industrial Technology (ICIT), 2015, pp. 738-744, doi: 10.1109/ICIT.2015.7125186.
- [24] H. S. Patel and R. G. Hoft, "Generalized harmonic elimination and voltage control in thyristor inverters: Part I- Harmonic elimination", IEEE Trans. Ind. Appl., Vol. IA-9, No. 3, pp. 310-31, May/Jun. 1973.
- [25] L. M. Tolbert, F. Z. Peng, and T. G. Habetler, "Multilevel converters for large electric drives," IEEE Trans. Ind. Applicant., vol. 35, no. 1, pp. 36-44, Feb. 1999.
- [26] J. Chiasson, L. M. Tolbert, K. McKenzie, and Z. Du, "Eliminating harmonics in a multilevel inverter using resultant theory," in Proceedings of the IEEE Power Electronics Specialists Conference, pp. 503-508, June 2002. Cairns, Australia.
- [27] J. Chiasson, L. M. Tolbert, K. McKenzie, and Z. Du, "Control of a multilevel converter using resultant theory," IEEE Transactions on Control System Technology, vol. 11, pp. 345-354, May 2003.
- [28] A. Kavousi, B. Vahidi, R. Salehi, M. K. Bakhshizadeh, N. Farokhnia, and S. H. Fathi, "Application of the bee algorithm for selective harmonic elimination strategy in multilevel inverters," IEEE Trans. Power Electron., vol. 27, no. 4, pp. 1689-1696, Apr. 2012
- [29] Z. Yuan, R. Yuan, W. Yu, J. Yuan, J. Wang, "A Groebner Bases Theory-Based Method for Selective Harmonic Elimination," IEEE Trans. Power Electron., vol. 30, no. 12, pp. 6581-1692, Dec. 2015
- [30] H. R. Baghaee, A. K. Kaviani, M. Mirsalim, G. B. Gharehpetian, "Harmonic optimization in single DC source multilevel inverters using RBF neural networks," Power Electron. and Drive Syst. Tech. Conf. (PEDSTC), Tehran, Iran, Feb. 2012, pp. 403 - 409.

- [31] B. Majidi, H. R. Baghaee, G. B. Gharehpetian, J. Milimonfared, M. Mirsalim, "Harmonic optimization in multi-level inverters using harmony search algorithm," IEEE 2nd Int. Power and Energy Conf., Malaysia, 2008, pp. 646 – 650.
- [32] B. Ozpineci, L. M. Tolbert, and J. N. Chiasson, "Harmonic optimization of multilevel converters using genetic algorithms," IEEE Power Electron. Lett., vol. 3, no. 3, pp. 92–95, Sep. 2005.
- [33] H. Taghizadeh and M. Tarafdar Hagh, "Harmonic elimination of multilevel inverters using particle swarm optimization," in Proc. IEEE Int. Symp. Ind. Electron., 2008, pp. 393–396.
- [34] M. Etesami, N. Farokhnia, and S. Fathi, "Colonial competitive algorithm development toward harmonic minimization in multilevel inverters," IEEE Trans. Ind. Inform., vol. 11, no. 2, pp. 459 - 466, Apr. 2015.
- [35] M. S. A. Dahidah, G. Konstantinou, N. Flourentzou, and V. G. Agelidis, "On comparing the symmetrical and non-symmetrical selective harmonic elimination pulse-width modulation technique for two-level three-phase voltage source converters," IET Power Electron., vol. 3, pp. 829-842, Nov. 2010.
- [36] M. S. A. Dahidah and V. G. Agelidis, "Non- symmetrical SHEPWM technique for five-level cascaded converter with non-equal DC sources," IEEE 2nd Int. Power and Energy Conf., Malaysia, 2008, pp. 775-780.
- [37] A. Tripathi and G. Narayanan, "Investigations on optimal pulse-width modulation to minimize total harmonic distortion in the line current," 2014 IEEE 6th India International Conference on Power Electronics (IICPE), Kurukshetra, 2014, pp. 1-6.
- [38] A. Tripathi and G. Narayanan, "Optimal PWM for minimization of current harmonic distortion in three-level inverter fed induction motor drives," 2016 IEEE International Conference on Power Electronics, Drives and Energy Systems (PEDES), Trivandrum, 2016, pp. 1-6.
- [39] G. Narayanan and V. T. Ranganathan, "Synchronized PWM Strategies Based on Space Vector Approach. Part 1: Principles of waveform Generation," IEE Proc. Elec. Power Appl., Vol. 146, No. 3, May 1999, 267-275.
- [40] Z. Liu, X. Zhang, M. Su, Y. Sun, H. Han and P. Wang, "Convergence Analysis of Newton-Raphson Method in Feasible Power-Flow for DC Network," in IEEE Transactions on Power Systems, vol. 35, no. 5, pp. 4100-4103, Sept. 2020, doi: 10.1109/TPWRS.2020.2986706.
- [41] G. S. Buja and G. B. Indri, "Optimal Pulse-Width Modulation for Feeding AC Motors," IEEE Trans. Ind. Appl. Vol. Ia- 1 3. No. 1. Jan/Feb 1977, pp. 38-44.
- [42] N. Yosefpoor, S. Fathi, N. Farokhina, and A. Abyaneh, "Thd minimization applied directly on the line-to-line voltage of multilevel inverters," IEEE Trans. Ind. Electron., vol. 59, no. 1, pp. 373-380, Jan 2008.
- [43] V. G. Agelidis, A. I. Balouktsis, and C. Cossar, "On attaining the multiple solutions of selective harmonic elimination pwm three-level waveforms through function minimization," IEEE Trans. on Ind. Electron., vol. 55, no. 3, pp. 996-1004, March 2008.
- [44] A. K. Rathore, J. Holtz, and T. Boller, "Synchronous optimal pulse width modulation for low-switching-frequency control of medium-voltage multilevel inverters," IEEE Trans. on Ind. Electron., vol. 57, no. 7, pp. 2374-2381, July 2010.
- [45] M. S. A. Dahidah and V. G. Agelidis, "Selective harmonic elimination PWM control for cascaded multilevel voltage source converters: A generalized formula," IEEE Trans. Power Electron., vol. 23, no. 4, pp. 1620–1630, Jul. 2008.
- [46] Amnesh Goel, Rakesh Kumar Bhujade "A Functional Review, Analysis and Comparison of Position Permutation Based Image Encryption Techniques", International Journal of Emerging Technology and Advanced Engineering, Volume 10, Issue 07, July 2020.
- [47] S. S. Lee, B. Chu, N. Rumzi, N. Idris, H. H. Goh and Y. E. Heng, "Switched-Battery Boost-Multilevel Inverter with GA Optimized SHEPWM for Standalone Application," IEEE Trans. Ind. Electron., vol. 63, no. 4, pp. 2133–2142, April, 2016.
- [48] N. Rai, A. Maheshwari and B. Rai, "Evaluation and Minimization of Total Harmonic Distortion in Two Level Voltage-Source Inverter Fed Induction Motor Drives," 2018 International Conference on Current

Trends towards Converging Technologies (ICCTCT), Coimbatore, 2018, pp. 1-7.

- [49] A. Tripathi and G. Narayanan, "Influence of three-phase symmetry on pulsating torque in induction motor drives," 2016 7th India International Conference on Power Electronics (IICPE), Patiala, 2016, pp. 1-6.



© 2022 by the M. Chaitanya Krishna Prasad, Dr. Vinesh Agarwal and Dr. Ashish Maheshwari. Submitted for possible open access publication under the terms and conditions of the Creative Commons Attribution (CC BY) license (<http://creativecommons.org/licenses/by/4.0/>).